



VISUALIZATION OF BUOYANCY-DRIVEN INSTABILITIES IN REACTIVE SYSTEMS

C. Almarcha^{1,4,c}, P. Grosfils², F. Dubois³, A. De Wit⁴

¹IRPHE, UMR 7342, CNRS, Aix-Marseille Univ., 49, rue F. Joliot Curie, 13013 Marseille, France

²Center for Nonlinear Phenomena and Complex Systems, Université Libre de Bruxelles (ULB), CP231, 1050 Brussels, Belgium.

³Microgravity Research Center, Chimie Physique E.P. CP 165/62, Université Libre de Bruxelles (ULB), Avenue F.D. Roosevelt 50, 1050 Brussels, Belgium

⁴Nonlinear Physical Chemistry Unit, ULB, CP231, 1050 Brussels, Belgium.

^cCorresponding author: Tel.: +33413552025; Fax: +33413552001; Email: Almarcha@irphe.univ-mrs.fr

KEYWORDS:

Main subjects: Experimental and computational fluid mechanics, reactive flows

Fluid: acid-base reactive flows

Visualization method(s): Schlieren, interferometry, particle image velocimetry

Other keywords: image processing, color indicator

ABSTRACT:

The study of buoyancy-driven instabilities triggered by chemical reactions has gained renewed interest because of their implications in CO₂ sequestration techniques among others. The theoretical models describing the evolution of the unstable interface between two miscible solutions, each containing a reactant, have to be compared to laboratory-scale experiments. We expose the diverse visualization methods we used to experimentally study the related buoyancy-driven instabilities of chemical fronts and their possible influence on the dynamics. This way, quantitative comparisons with numerical simulations give good agreements.

INTRODUCTION:

Chemical reactions and buoyancy-driven instabilities can often interplay in fluid dynamics. For instance, in the specific case of CO₂ sequestration in the ground or in aquifers, chemical reactions induce changes in the properties of the fluids (changes in the density or in the viscosity), or eventually in the properties of the porous medium (changes in the porosity). In turn, related hydrodynamic instabilities change the mixing of reactants and the yield of the reaction.

We present here the techniques to use or to avoid when experimentally studying the dynamics resulting from the coupling between chemical reactions and hydrodynamic instabilities. More specifically, we focus here on buoyancy-driven instabilities in porous media, for which the buoyant flows are of particular importance for mixing in the absence of any external forcing flow. Therefore, we use a Hele-Shaw cell (Figure 1 left), i.e. two glass plates separated by a thin gap width, that allows quantitative comparisons with two-dimensional numerical models of porous media. Two miscible solutions, each containing a reactant A or B, are put into contact, one above the other [1]. By diffusion and convection, species A and B meet and the reaction $A+B \rightarrow C$ produces species C (Figure 1 right). The buoyancy-driven instabilities result from the gradients of density in the gravity field. In the absence of reaction, three types of instability can appear [2]. The Rayleigh-Taylor instability (RT) is known to appear when a denser fluid is put on top of a less dense one. Double-diffusive (DD) fingering and diffusive layer convection (DLC) instabilities develop when the upper solute and the lower solute diffuse at different rates. In presence of reactions, the number of possible scenarios increases up to 32. To tackle and analyze these various cases, experimental investigation is necessary. In order to get a maximum of quantitative results, visualizations techniques must be accurate. We emphasize this with the example of an acid base reaction between HCl and NaOH solutions [3-7].



1. EXPERIMENTAL SYSTEM:

The experiments are performed in a vertically oriented Hele-Shaw cell specifically designed to create a planar interface between two solutions [1]. The gap width is typically 0.5mm. The upper layer is filled from a hole made on top of the cell, and the bottom layer is filled from a hole at the bottom of the cell (in green on Figure 1). Two exhaust holes are situated on the middle right and middle left of the cell (in red on Figure 1). They aim at evacuating the excess of liquid, and at defining the initial condition of a flat interface between the two reactants. This is done by first imposing a flux of solution from top and bottom (arrows on Figure 1). Upper and lower solutions meet on a line along the exhaust hole and the stagnation point in the middle of the cell. The experiment starts when the injection fluxes are stopped. We then let the system evolve from this situation. The thickness of the initial mixing zone between the two reactants depends on the initial flux, as a competition between advection and diffusion at the stagnation point.

The reaction chosen is the neutralization reaction between HCl and NaOH in aqueous solutions. As they are strong acid and base, they are fully dissociated in the solution. Due to electroneutrality, we consider that ions go by pair. So species A is chosen to be the H^+/Cl^- couple and species B is the Na^+/OH^- couple. The product C is Na^+/Cl^- . The reaction-diffusion evolution of the species in the absence of convection is reported on Figure 1 right.

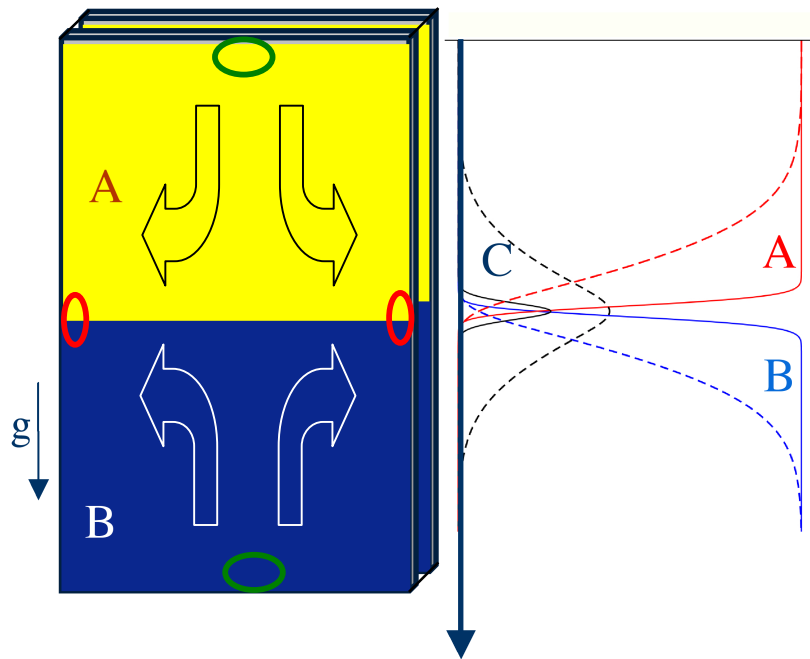


Fig.1: Left: Sketch of the vertically oriented Hele Shaw cell filled with an upper solution (in yellow) and a lower solution (in blue). The cell is filled through holes (in green). The excess is evacuated thanks to two exhaust holes (in red). Right: Sketch of the reaction-diffusion concentration profiles of solutes A and B at two different times.



2. VISUALISATION TECHNIQUES:

As the solutions are transparent and colorless, the first idea would be to use a color indicator to track the pH variations and the reaction zone. Unfortunately, we show in section 2.5 that the color indicator, as a reacting species, can modify the dynamics of the system and the resulting pattern [6,7]. This is why we first present non-intrusive techniques.

2.1 SCHLIEREN TECHNIQUE:

The variations in concentrations and temperature modify the local optical index. The contributions are $0.0083 \text{ l mol}^{-1}$ for HCl, $0.0098 \text{ l mol}^{-1}$ for NaOH, $0.0106 \text{ l mol}^{-1}$ for NaCl and 0.001 K^{-1} for temperature (from ref. 8). As a consequence, we used a Toepler's single-field-lens schlieren arrangement [9]. The knife edge was put horizontal, to visualize the gradients in the vertical direction. An example for a molar solution of HCl on top of a molar solution of NaOH is reported on Fig. 2. We clearly see the emergence of fingers, as an evidence of convection, in the upper layer only [3,4]. The reaction front, i.e. the zone of coexistence of reactants, is visible as a thin flat horizontal line separating on the bottom the dark and white zones.

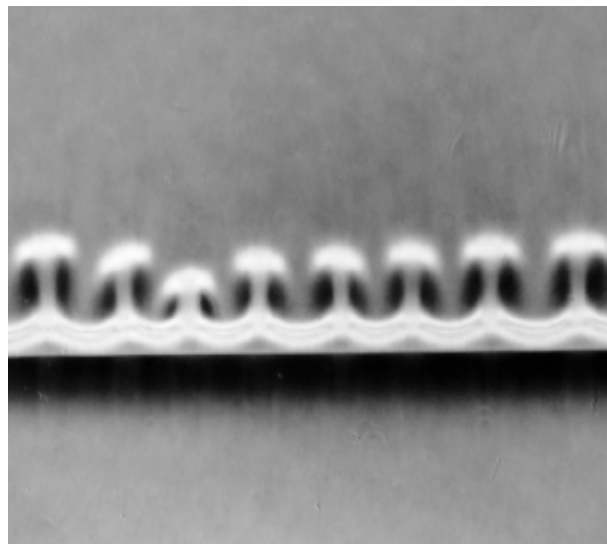


Fig.2: Visualization of the pattern induced by putting a 1M HCl solution on top of 1M NaOH solution. The field of view is 24 mm large.

2.3 INTERFEROMETRY:

In order to get a more quantitative description of the pattern, we use a Mach-Zehnder interferometer (Fig.3) [3,10]. The source is a 633 nm Laser beam. The image is recorded by a CCD camera. An example of interferogram, at two different times, is reported on Figure 4. The fringes, vertical in a homogeneous medium, are shifted by the refractive index variations. The demodulation by a Fourier transform algorithm [11] leads to the variations of the refractive index reported on figure 5. The absolute value of the refractive index has been fixed on the upper solution according to values found in ref. 5.

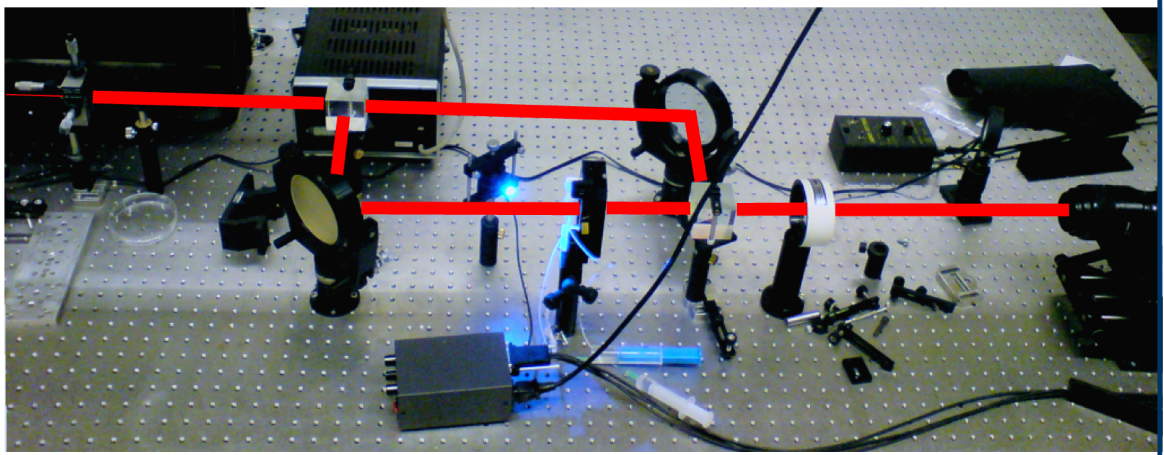


Fig.3: Mach-Zehnder interferometer set-up. In the center, the Hele Shaw cell, alternatively illuminated by the white led for PIV measurements.

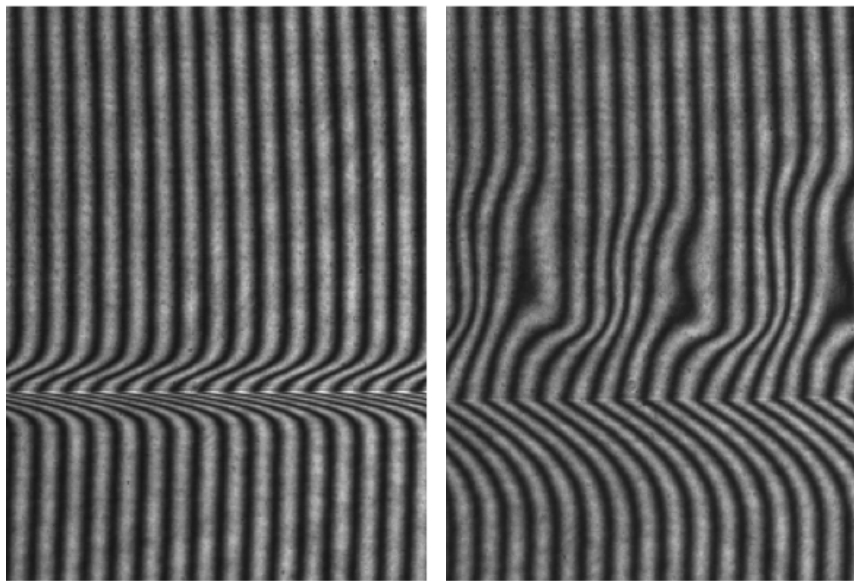


Fig.4: Interferograms at the beginning of the experiments (left) and after fingers are developed (right). The field of view is 8 mm large.

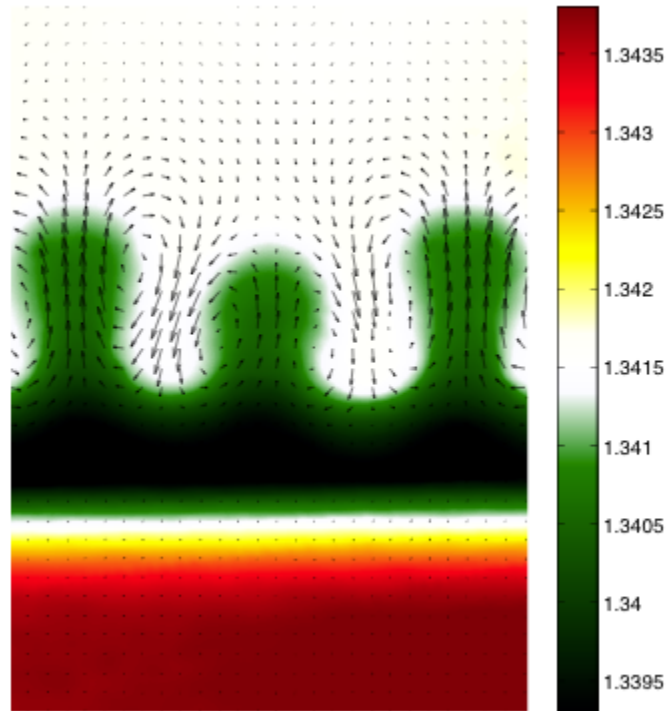


Fig.5: Refractive index map, reconstructed from the interferogram in Figure 4. The PIV vector field is also reported. The field of view is 8 mm large.

2.4 PIV TECHNIQUE:

In alternance with the interferometry measure, we seeded the solution with 5 microns latex particles and illuminated in volume with a white led. The images have been recorded on the same camera as the interferogram (see fig. 6). This way, we obtained the PIV and interferograms at the same times. The velocity field has been calculated using the free software DPIVsoft [12]. On figure 5, the velocity field has been superimposed on the optical index map.

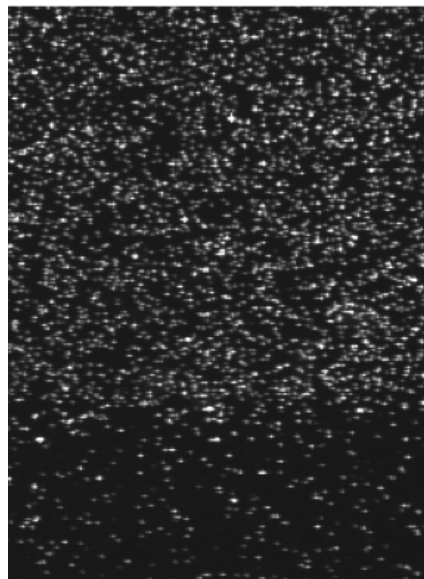


Fig.6: The solutions are seeded with 5 microns latex particles. The field of view is 8 mm large.



2.5 USE OF COLOR INDICATOR:

In order to visualize the reaction front in a direct way, color indicators are often used. Unfortunately, this technique is risky because the color indicator is a chemical reactant that can interfere with the other species and contribute to modify the density profile. As an example, in the work reported on ref. 6 and 7, Green Bromocresol was used. The acidic form of this color indicator is yellow while its basic form is blue. The interplay of this color indicator with the HCl-NaOH reaction can modify the acid-base equilibrium and perturb the concentrations and density gradients. Hence, as the acidic and basic forms of the color indicator don't have the same solutal expansion coefficient, buoyancy-driven instabilities can appear just because of the presence of the color indicator. On figure 7, we reproduced the experiment of the contact between HCl and NaOH 0.01M solutions but in the presence of 0.01M Green Bromocresol. Although the zone of pH transition is visible (in black), we see also the emergence of fingers in the lower solution. A comparison with Figs.2 where fingers are seen only at the top proves that the color indicator has indeed modified the dynamics. More explanations on the influence of the color indicator can be found in Refs. 6 and 7.

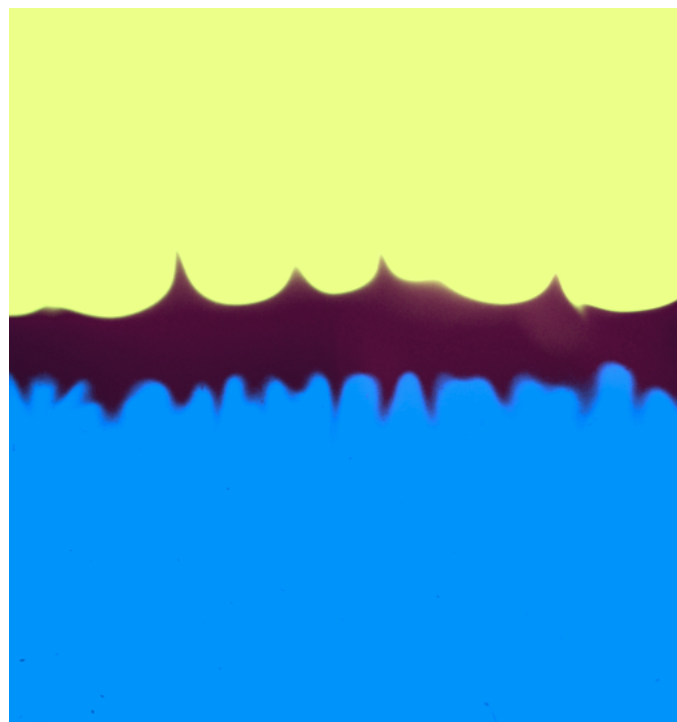


Fig.7: Direct visualization of the pattern for a 0.01M HCl solution with color indicator on top of 0.01M NaOH solution with color indicator Bromocresol Green. Fingers are observed in the lower layer as well. The field of view is 30 mm large.

3. RESULTS AND CONCLUSION:

In order to confirm the experimental results from the interferometry and PIV visualizations, we have numerically integrated a two dimensional model for flows in porous media where Darcy's law is coupled to reaction-diffusion-convection equations for the concentration of each species [3]. The parameters in the simulations were taken from ref. 8. The results are reported on figure 8 for the same time and scale as in figure 5. We clearly see a good agreement between numerical simulations and experiments. We can conclude that the interferometry and PIV techniques are well suited to study the buoyancy-driven instabilities in Hele Shaw cells, as a model of 2D porous media while the use of color indicators should be avoided.

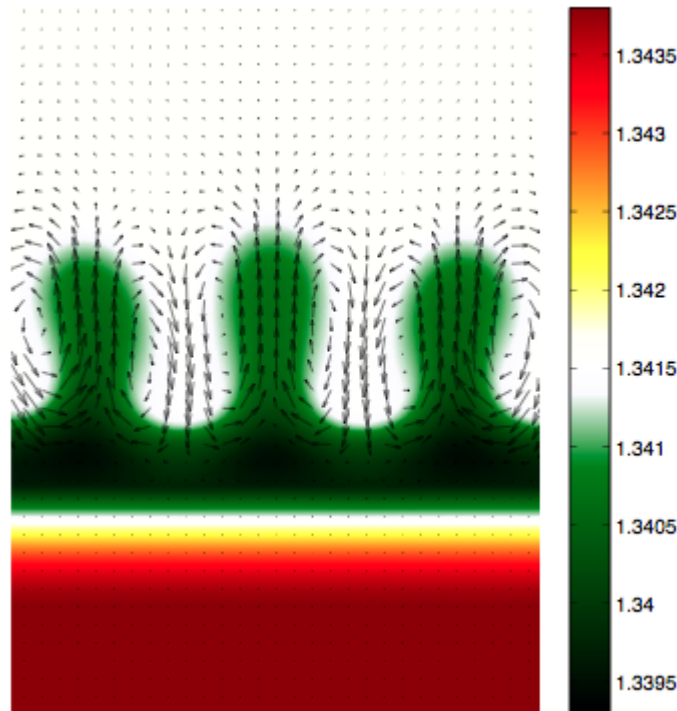


Fig.8: Optical refractive index variations and PIV vector field obtained from direct numerical simulation. To be compared to Fig.5.

References

1. Shi Y., Eckert K., *A novel Hele-Shaw cell design for the analysis of hydrodynamic instabilities in liquid-liquid systems*, Chem. Eng. Sci., 2008, **63**, 3560-3563.
2. Trevelyan P.M.J., Almarcha C., De Wit A., *Buoyancy-driven instabilities of miscible two-layer stratifications in porous media and Hele-Shaw cells*, J. Fluid Mech., 2011, **670**, 38-65.
3. Almarcha C., Trevelyan P.M.J., Grosfils P., De Wit A. *Chemically driven hydrodynamic instabilities*. Phys. Rev. Lett. 2010, **104**, 044501.
4. Almarcha C., R'Honi Y., De Decker Y., Trevelyan P.M.J., Eckert K., De Wit A. *Convective mixing induced by acid-base reactions*. J. Phys. Chem. B 2011, **115**, 9739-9744.
5. Zalts A., El Hasi C., Rubio D., Urena A., D'Onofrio A., *Pattern formation driven by an acid-base neutralization reaction in aqueous media in a gravitational field*, Phys.Rev. E, 2008, **77**, 015304.
6. Almarcha C., Trevelyan P.M.J., Riolfo L.A., Zalts A., El Hasi C., D'Onofrio A., De Wit A. *Active Role of a Color Indicator in Buoyancy-Driven Instabilities of Chemical Fronts*. J. Phys. Chem. Lett. 2010, **1**, 752-757.
7. Kuster S., Riolfo L.A., Zalts A., El Hasi A., Almarcha C., Trevelyan P.M.J., De Wit A. and D'Onofrio A., *Differential diffusion effects on buoyancy-driven instabilities of acid-base fronts: the case of a color indicator*, Phys. Chem. Chem. Phys., 2011, **13**, 17295-17303.
8. *CRC Handbook of Chemistry and Physics*, 59th ed., edited by Robert C. Weast. CRC, Boca Raton, Florida, 1979.
9. G.S. Settles, *Schlieren and shadowgraph techniques*, Springer, 2001.
10. Grosfils P., Dubois F., Yourassowsky C., De Wit A., *Hot spots revealed by simultaneous experimental measurement of the two-dimensional concentration and temperature fields of an exothermic chemical front_during finger-pattern formation*, Phys. Rev. E, 2009, **79**, 017301.
11. Takeda M., Ina H., Kobayashi S., *Schlieren and shadowgraph techniques*, J. Opt. Soc. Am. 1982, **72**, 156.
12. Meunier P., Leweke T., *Analysis and treatment of errors due to high velocity gradients in particle image velocimetry*, Exp. Fluids 2003, **35**, 408.